

Cosmic Rays, Radio Halos and Non-Thermal X-ray Emission in Clusters of Galaxies

Pasquale Blasi^a and Sergio Colafrancesco^b

^a*Dept. of Astronomy & Astrophysics, E. Fermi Inst., University of Chicago, Chicago, IL 60637-1433, USA*

^b*Osservatorio Astronomico di Roma, Via dell'Osservatorio 2, I-00040 Monteporzio, Italy*

Abstract

We calculate the flux of radio, hard X-ray and UV radiation from clusters of galaxies as produced by synchrotron emission and Inverse Compton Scattering of electrons generated as secondaries in cosmic ray interactions in the intracluster medium. Both the spatial distribution of cosmic rays due to their diffusion and the spatial distribution of the intracluster gas are taken into account.

Our calculations are specifically applied to the case of the Coma cluster. The fluxes and spectra of the radio halo emission and of the hard X-ray excess from Coma can be explained in this model if an average magnetic field $B \sim 0.1\mu G$ is assumed. However, such a low value for the intracluster magnetic field implies a large cosmic ray energy density which in turn is responsible, through neutral pion decay, for a gamma ray flux above 100 MeV which exceeds the EGRET upper limit. This gamma ray bound can be relaxed if the hard X-ray excess and the radio halo emission from Coma are not due to the same population of electrons.

We finally stress the unique role that the new generation gamma ray satellites will play to discriminate among different models for the non thermal emission in clusters of galaxies.

1 Introduction

The origin of the non-thermal, diffuse emission (radio, X-ray and UV) in galaxy clusters still remains poorly understood. The general consensus is that the radio and X-ray non-thermal emission are likely to be produced by a population of relativistic electrons via synchrotron emission and Inverse Compton Scattering (hereafter ICS) off the Microwave Background photons, respectively. However, the origin, acceleration and propagation of these relativistic

electrons are still subject to debate. If electrons are accelerated in discrete sources in the central regions of clusters, the severe energy losses and the diffusive motion force the electrons to cover at most distances of order of a few kpc from the source, while diffuse radio emission is clearly observed on Mpc scales [1]. To solve this problem, reacceleration models have been invoked (see [2] for a discussion), though the nature of the *in situ* acceleration is not yet completely clear.

A natural solution to the problem mentioned above was first proposed in [3] and [4], where the electrons responsible for the non-thermal emission were produced *in situ* as secondary products of cosmic ray nucleons interacting with the protons in the intracluster medium (hereafter ICM). Cosmic rays (hereafter CR) in clusters of galaxies are, in fact, practically free from energy losses and can reach large distances from the source. An interesting consequence of this model is that not only electrons but also gamma rays (through the decay of neutral pions) and neutrinos are also produced in the same interactions [5–7]. We show here that this point can strongly constrain the validity of the secondary electron model (hereafter SEM) as the explanation of the diffuse, non-thermal emission from galaxy clusters. The SEM in his original version [3,4] was recently questioned [8] as the explanation of the diffuse radio halo of Coma, because of the too steep CR spectrum [$Q(E) \sim E^{-(2.5-2.7)}$] required to fit the data.

The aim of this paper is to calculate the flux and the spectra of the non-thermal radio, UV and hard X-ray emission from Coma in the framework of the SEM, addressing the following points, not considered in previous works:

i) the calculations in [3,4,8] are all carried out in the assumption that CR are permanently confined in the cluster volume. Indeed, as shown in [6] and [7] this is true only for CR with energy below a *confinement energy* E_c (see Section 2 below), which depends quite strongly on the diffusion coefficient in the ICM;

ii) in previous calculations [3,4,8], a spatially homogeneous equilibrium distribution of CR was always assumed. However, if CR are mainly contributed by a small number of discrete powerful sources in the cluster core (as it seems to be the case in Coma), the distribution of CR due to diffusion is strongly inhomogeneous (for instance in the case of a single source the CR distribution goes as $1/r$ if r is the distance to the source). Similar conclusions hold in case of shocks produced by (sub)cluster merging or during the cluster collapse, as sources of CR in the clusters. We consider here both the cases of a single source and of a spatially homogeneous injection of CR in the ICM;

iii) the observable fluxes of non-thermal radiation are calculated as a convolution of the distribution of CR and of the targets for CR interactions, which

are provided by the IC gas protons. Therefore the spatial distribution of the IC gas, never considered in previous calculations, can have a relevant role and needs to be considered;

iv) in the previous works [3,4,8] a quite steep spectrum, $J(\nu) \sim \nu^{-1.34}$, for the Coma radio halo was considered for the comparison with the model predictions. This was the main reason to call for a correspondingly steep CR spectrum and eventually claim to rule out the SEM [8]. However recent observations (see, e.g., [1]) show that the radio spectrum from Coma is well fitted by a power law with power index ~ 1.16 up to a frequency 1.4 GHz, while there is a still controversial evidence for a steepening at higher frequencies (see [9] [10]; see also [1] for a review).

v) we use here a detailed treatment for the pp collisions, which is particularly important in the calculation of the fluxes of gamma and UV radiation from clusters of galaxies.

In addition to the points listed above, there are some recent data that introduce new limits on the SEM. In particular, the combination of the EGRET limit on the gamma ray emission from Coma [11] and the recent detection of an hard X-ray non-thermal tail above 20 keV from Coma, obtained by the SAX [12] and the RXTE [13] experiments, allows us to strongly constrain the validity of the SEM as a combined explanation of both the radio halo emission and the hard X-ray excess. Furthermore, we also consider the still debated evidence of a diffuse UV emission from Coma [14,10] as a possible indication of ICS emission from very low energy electrons.

The structure of the paper is the following: in Section 2 we discuss the CR propagation in clusters of galaxies; in Section 3 we derive the secondary electron spectrum from CR collisions in the ICM. We present our calculations for the non-thermal, diffuse radio and X-ray emission in Section 4.1 and 4.2, respectively. In Section 4.3 we also derive the expected gamma-ray flux produced by the same CR interactions responsible for the secondary electrons. In Section 5 the calculations are applied and discussed in the case of Coma. Our conclusions are presented in the final Section 6. Throughout the paper we use an dimensionless Hubble parameter $h = (H_0/100 \text{ km s}^{-1} \text{ Mpc}^{-1}) = 0.6$ and $\Omega_0 = 1$, unless otherwise specified.

2 Cosmic ray propagation in the intracluster medium

Following [6,7], we first assume that the accelerated CRs in clusters are mainly supplied by radio galaxies – or more generally by active galaxies – and/or by the possible shocks occurring predominantly in the central regions of galaxy

clusters. As estimated in [6,7] we can expect nearly one of these active galaxies per rich cluster, on average, and also we can expect that there is at least one major shock after its formation [15] in the central regions of the clusters. Actually, this seems to be the situation in the Coma cluster (see [16]). For simplicity, we consider here a CR source in the central region of the cluster irrespective of its peculiar nature. We will also discuss the more general case of an extended distribution of cluster CR sources in a forthcoming paper [17]. In the end of this section we consider the case of a spatially homogeneous injection of CR as an extreme case opposite to that of a single source.

In the typical magnetic fields present in clusters of galaxies (see [18] and [19] for reviews), the propagation of CR is diffusive and can be described by the transport equation:

$$\frac{\partial n_p(E_p, r, t)}{\partial t} - D(E) \nabla^2 n_p(E_p, r, t) - \frac{\partial}{\partial E_p} [b(E_p) n_p(E_p, r, t)] = Q(E_p) \delta(\vec{r}), \quad (1)$$

where $n_p(E_p, r, t)$ is the density of CRs with energy E_p at distance r from the source, $Q_p(E_p) = Q_0 p_p^{-\gamma}$ [with $p_p = (E_p^2 - m_p^2)^{1/2}$ being the proton momentum] is the assumed spectrum of the CR source and $b(E_p)$ is the rate of energy losses. The normalization constant, Q_0 , is related to the CR luminosity, L_p , by

$$Q_0 \int_0^{E_p^{max}} dT_p T_p p_p^{-\gamma} = L_p ,$$

where $T_p = E_p - m_p$ is the kinetic energy of the proton. The diffusion coefficient, $D(E_p)$, has been explicitly assumed to be independent of r because we consider an average magnetic field uniformly distributed in the ICM. As for the diffusion coefficient, we adopted the same approach as in [7]. Specifically, we assume that the spectrum of the fluctuations in the IC magnetic field is described by a Kolmogorov spectrum, $P(k) = P_0(k/k_0)^{-5/3}$, and we use the following expression to relate the diffusion coefficient $D(E_p)$ to $P(k)$:

$$\begin{aligned} D(E_p) &= \frac{1}{3} r_L c \frac{B^2}{\int_{1/r_L}^{\infty} dk P(k)} \\ &= 2.3 \times 10^{29} E_p (\text{GeV})^{1/3} B_\mu^{-1/3} \text{cm}^2/\text{s} \left(\frac{l_c}{20 \text{kpc}} \right)^{2/3} . \end{aligned} \quad (2)$$

Here r_L is the Larmor radius of the particles with energy E_p and B is the rms magnetic field strength (B_μ is its value expressed in μG). The normalization constant P_0 is obtained requiring that the total energy density in the field equals B^2 . Here $l_c \approx 1/k_0$ is the size of the largest eddy in the magnetic field.

In clusters of galaxies eq. (1) simplifies appreciably because the term of energy losses can be neglected. In fact, for a typical rich cluster with IC gas mass, $M_{gas} \simeq 10^{14} M_{\odot}$, and total mass, $M_{tot} \sim 10^{15} M_{\odot}$, over a distance comparable with the Abell radius $R_A = 1.5/h$ Mpc, the average IC gas density turns out to be $\bar{n}_H \sim 3 \cdot 10^{-4} \text{ cm}^{-3} h^2$, which corresponds to a column density of $\sim 6 \text{ g/cm}^2 \ll x_{nucl} = (m_p/\sigma_{pp}) \approx 50 \div 100 \text{ g/cm}^2$ (here $\sigma_{pp} \approx 3 \times 10^{-26} \text{ cm}^2$ is the cross section for pp collisions and m_p is the proton mass). This estimate is found assuming CR confined in the cluster for times comparable with the cluster age. For non confined CR, the IC gas column density is even lower.

In this framework, the solution of eq.(1) found at the present time, t_0 , after the source started to produce CR is given by:

$$n_p(E_p, r) = \frac{Q_p(E_p)}{D(E_p)} \frac{1}{2\pi^{3/2}r} \int_{r/r_{max}(E_p)}^{\infty} dy e^{-y^2}, \quad (3)$$

where the source term has been assumed active for all the age, t_{cl} of the cluster (which is comparable, for our purposes, to the age, t_0 , of the universe).

We introduce the quantity $r_{max}(E_p) = \sqrt{4D(E_p)t_0}$ which represents the average maximum distance that a particle with energy E_p can diffuse away from the source in the time t_0 . If $r \ll r_{max}(E_p)$, then the lower limit in the integral in eq.(3) above is small and eq.(3) gives the well known stationary solution:

$$n_p(E_p, r) = \frac{Q_p(E_p)}{D(E_p)} \frac{1}{4\pi r}. \quad (4)$$

At distances larger than $r_{max}(E_p)$ the density of particles with energy $\leq E_p$ is suppressed.

If R_H is the confinement size of a cluster (here we consider $R_H \sim$ the radio halo size), then the solution of the equation $r_{max}(E_c) = R_H$ gives an estimate of the maximum energy, $E_c \sim (R_H^2/4D_0t_0)^{1/\eta}$, for which CRs are confined inside the cluster. Thus, particles with energy lower than E_c need times larger than t_0 to leave the cluster, and particles with energy larger than E_c diffuse away from the cluster in the time $\sim R_H^2/4D(E_p)$. In other words, clusters of galaxies can be considered as *closed boxes* only for CRs having energy $E_p \lesssim E_c$ [6,7].

Finally, we discuss here also the extreme case of a homogeneous injection of CR in the ICM. In this case the equilibrium CR distribution is simply given by

$$n_p(E_p) = K \frac{\epsilon_{tot}}{V} p_p^{-\gamma} \quad (5)$$

where again the constant K is obtained requiring that

$$K \int_0^{E_p^{max}} dT_p T_p p_p^{-\gamma} = \epsilon_{tot} ,$$

and ϵ_{tot} is the total energy injected in the cluster volume V in the form of CR. This neglects the leaking of CR from the boundary of the cluster, which is equivalent to assume that the relevant CR are confined in the cluster. This assumption is justified, because even if CR with high energy do escape, they do not appreciably affect the energy balance in the cluster for injection spectra steeper than E_p^{-2} at high energy. Note that eq. (5) is no longer valid close to the cluster boundary.

3 Secondary electrons in pp collisions

CRs interact with the IC gas protons and produce electrons (e^+e^-), neutrinos and gamma rays through the decays of charged and neutral pions, respectively (see, e.g., [6,7]). In this section we concentrate on the electron component which is relevant for the calculations of the radio, UV and hard X-ray emission.

The spectrum of secondary electrons with energy E_e at distance r from the CR source is readily calculated by convolution of the proton, pion and muon spectra and is given by:

$$q_e(E_e, r) = \frac{m_\pi^2}{m_\pi^2 - m_\mu^2} n_H(r) c \cdot \int_{E_e}^{E_p^{max}} dE_\mu \int_{E_\pi^{min}}^{E_\pi^{max}} dE_\pi \int_{E_{th}(E_\pi)}^{E_p^{max}} dE_p F_\pi(E_\pi, E_p) F_e(E_e, E_\mu, E_\pi) n_p(E_p, r) , \quad (6)$$

where E_p^{max} is the maximum proton energy (note that our calculations are insensitive to the exact value of E_p^{max}), $E_{th}(E_\pi)$ is the threshold energy for the production of pions with energy E_π and we put

$$E_\pi^{min} = \frac{2E_\mu}{(1 + \beta) + \xi(1 - \beta)} ; \quad E_\pi^{max} = \min \left\{ E_p^{max}, \frac{2E_\mu}{(1 - \beta) + \xi(1 + \beta)} \right\} ,$$

where $\xi = m_\pi^2/m_\mu^2$ and β is the velocity of muons in units of the light speed. The quantity $n_p(E_p, r)$ is the equilibrium CR spectrum at distance r from the source, as given by eq. (3) for a single CR source or from eq. (5) in the case of a homogeneous CR injection. The quantity $n_H(r)$ is the density profile of

the IC gas as a function of the radial distance from the cluster center and is well fitted by a King profile, $n_H(r) = n_H^0 \left[1 + \left(\frac{r}{r_0} \right)^2 \right]^{-3\beta_{IC}/2}$, where n_H^0 is the central IC gas density, r_0 is the core radius and β_{IC} is a phenomenological parameter in the range $0.7 \lesssim \beta_{IC} \lesssim 1.1$ (see [20] for a review).

The physics of the interaction is contained in the functions $F_\pi(E_\pi, E_p)$ (the spectrum of pions produced in a CR interaction at energy E_p in the laboratory frame) and $F_e(E_e, E_\mu, E_\pi)$ (the spectrum of electrons from the decay of a muon of energy E_μ produced in the decay of a pion with energy E_π). The electron spectrum is given by the following expression:

$$F_e(E_e, E_\mu, E_\pi) = \frac{1}{\beta E_\mu} \times \left. \begin{array}{l} \left\{ \begin{array}{l} 2 \left(\frac{5}{6} - \frac{3}{2}\lambda^2 + \frac{2}{3}\lambda^3 \right) - P_\mu \frac{2}{\beta} \left[\frac{1}{6} - \left(\beta + \frac{1}{2} \right) \lambda^2 + \left(\beta + \frac{1}{3} \right) \lambda^3 \right] \quad \text{if } \frac{1-\beta}{1+\beta} \leq \lambda \leq 1, \\ \frac{4\lambda^2\beta}{(1-\beta)^2} \left[3 - \frac{2}{3}\lambda \left(\frac{3+\beta^2}{1-\beta} \right) \right] - \\ \frac{4P_\mu}{1-\beta} \left\{ \lambda^2(1+\beta) - \left[\frac{1}{2} + \lambda(1+\beta) \right] \frac{2\lambda^2}{1-\beta} + \frac{2\lambda^3(\beta^2+3)}{3(1-\beta)^2} \right\} \quad \text{if } 0 \leq \lambda \leq \frac{1-\beta}{1+\beta}, \end{array} \right\} \end{array} \right\} (7)$$

where we put

$$P_\mu = P_\mu(E_\pi, E_\mu) = \frac{1}{\beta} \left[\frac{2E_\pi\xi}{E_\mu(1-\xi)} - \frac{1+\xi}{1-\xi} \right], \quad (8)$$

and $\lambda = E_e/E_\mu$. The above expression for F_e takes into account that the muons produced from the decay of pions are fully polarized (this is the reason why the pion energy E_π appears in the expression for the electron spectrum from the muon decay).

Determining the pion distribution is not trivial in particular in the low energy region (pion energies close to the mass of the pions) where not many data are available. A satisfactory approach to the low energy pion production was proposed in [21] and recently reviewed in [22] in the context of the *isobaric model*. The detailed and lengthy expressions for F_π that we used are reported and discussed in details in [22] (see their Appendix). Thus, following [22], we use here their model for collisions at $E_p \lesssim 3$ GeV. For $E_p \gtrsim 7$ GeV we use the scaling approximation which can be formalized writing the differential cross section for pion production as

$$d\sigma/dE_\pi = (\sigma_0/E_\pi) f_{\pi^\pm}(x), \quad (9)$$

where $\sigma_0 = 3.2 \cdot 10^{-26} \text{ cm}^2$, $x = E_\pi/E_p$. The scaling function $f_{\pi^\pm}(x)$ is given

by

$$f_{\pi^\pm}(x) = 1.34(1-x)^{3.5} + e^{-18x}. \quad (10)$$

In this case the function F_π coincides with the definition of differential cross section given in eq. (9).

The electron spectrum rapidly reaches its equilibrium configuration mainly due to synchrotron and ICS energy losses at energies larger than ~ 150 MeV and mainly due to Coulomb energy losses at smaller energies. The equilibrium spectrum can be calculated solving the transport equation

$$-\frac{\partial}{\partial E_e} [n_e(E_e, r)b(E_e)] = q_e(E_e, r) \quad (11)$$

where $n_e(E_e, r)$ is the equilibrium electron distribution and

$$b_e(E_e) = \left(\frac{dE_e}{dt}\right)_{ICS} + \left(\frac{dE_e}{dt}\right)_{syn} + \left(\frac{dE_e}{dt}\right)_{Coul} = b_0(B_\mu)E_e^2 + b_{Coul}$$

is the rate of energy losses per unit time at energy E_e . Here, we put $b_0(B_\mu) = (2.5 \cdot 10^{-17} + 2.54 \cdot 10^{-18} B_\mu^2)$ and $b_{Coul} = 7 \times 10^{-16} n_H(r)$ (if b_e is given in units of GeV/s). In the expression for b_{Coul} , the IC gas density $n_H(r)$ is given in units of cm^{-3} .

4 Non thermal emission from galaxy clusters

In this section we derive the non-thermal radio, hard X-ray and gamma ray spectra of galaxy clusters as obtained in the context of the SEM for the case of a single CR source.

4.1 The diffuse radio emission

The calculation of the radio emissivity per unit volume is performed here in the simplified assumption that electrons with energy E_e radiate at a fixed frequency given by [23]:

$$\nu \approx 3.7 \cdot 10^6 B_\mu E_e^2 (GeV) Hz. \quad (12)$$

This approximation introduces negligible errors in the final result and has the advantage of making it of immediate physical interpretation.

The radio emissivity at frequency ν and at distance r from the cluster center can be calculated as

$$j(\nu, r) = n_e(E_e, r) \left(\frac{dE_e}{dt} \right)_{syn} \frac{dE_e}{d\nu}. \quad (13)$$

The observed flux of radio emission from the cluster is obtained by integration of $j(\nu, r)$ over the cluster volume. Though the numerical calculations have been carried out using the exact solution of eq.(3) for the CR equilibrium spectrum, some useful information can be extracted from the following simplified picture. Let us assume that at fixed proton energy, E_p , particles with energy larger than E_p are the only ones able to diffuse out to distances $r > r_{max}(E_p)$ [at first approximation this assumption is correct just by the definition of $r_{max}(E_p)$]. Let us also assume for simplicity a constant IC gas density, \bar{n}_H . Most of the electrons responsible for the radio emission are produced in CR interaction at energies in the scaling regime [eqs. (9-10)]. Within these assumptions it is straightforward to show that $j(\nu, r) \propto (1/r)\nu^{-(\gamma+\eta)/2}$ and that the integrated diffuse radio flux reads:

$$J(\nu) \propto \nu^{-(\gamma+\eta)/2} \int_0^{r_{max}(\nu)} dr r. \quad (14)$$

The electron energy and the radio frequency are related through eq. (12) and in this simplified approach we can assume that protons with energy $E_p \sim 10E_e$ produce electrons with energy E_e . This means that the distance $r_{max}(\nu)$ in eq. (14) is proportional to $\nu^{\eta/4}$ for collisions involving CR confined in the cluster, while it is simply equal to the confinement radius R_H for non confined CR. In the first case, the observed spectrum is $J(\nu) \propto \nu^{-\gamma/2}$, independent on the details of the diffusion (this is the same result highlighted in [6] and [7] for gamma rays) while, in the other case, the spectrum is steepened as $J(\nu) \propto \nu^{-(\gamma+\eta)/2}$ above a frequency ν^* which is dependent on the diffusion coefficient and on the spatial scale of the confinement region. The situation is indeed more complicated in any realistic case, but the main features and in particular the high frequency steepening are still present. In particular, the introduction of a realistic King profile for the IC gas density distribution in the cluster translates into a decrease of the effective frequency ν^* with respect to the case of a uniform IC gas distribution.

4.2 The diffuse, non-thermal X-ray and UV emissions

The relativistic electrons responsible for the radio halo emission also emit X-rays and UV photons through ICS off the Microwave Background photons. As

in the case of the synchrotron emission, also for ICS we adopt the approximation that electrons radiate at a single energy, given by

$$E_X = 2.7 \text{ keV } E_e^2(\text{GeV}). \quad (15)$$

Electrons with energy in excess of a few GeV radiate in the hard X-ray range, while electrons with energy smaller than ~ 400 MeV produce soft X-rays and UV photons.

The non-thermal X-ray/UV emissivity at distance r from the CR source is

$$\phi_X(E_X, r) = n_e(E_e, r) \left(\frac{dE_e}{dt} \right)_{ICS} \frac{dE_e}{dE_X}. \quad (16)$$

In complete analogy with the case of the radio emission, the integrated non-thermal X-ray flux, $\Phi_X(E_X)$ is

$$\Phi(E_X, r) = \int_0^{R_H} dr 4\pi r^2 \phi_X(E_X, r). \quad (17)$$

Considerations similar to those presented in the previous section hold for the steepening of the hard X-ray spectrum from ICS.

4.3 The gamma ray emission

Gamma ray emission from clusters of galaxies is mainly produced by the decay of neutral pions (see, e.g., [6,7]) and by bremsstrahlung emission of secondary electrons (note that also primary electrons contribute to the bremsstrahlung flux, so that the contribution calculated here is a lower limit).

The emissivity in gamma rays at distance r and energy E_γ is given by

$$j_\gamma^{\pi^0}(E_\gamma, r) = 2n_H(r)c \int_{E_\pi^{min}(E_\gamma)}^{E_p^{max}} dE_\pi \int_{E_{th}(E_\pi)}^{E_p^{max}} dE_p F_{\pi^0}(E_\pi, E_p) \frac{n_p(E_p, r)}{(E_\pi^2 + m_\pi^2)^{1/2}}, \quad (18)$$

where $E_\pi^{min}(E_\gamma) = E_\gamma + m_{\pi^0}^2/(4E_\gamma)$. We refer to [22] for the expression of $F_{\pi^0}(E_\pi, E_p)$ in the low energy collisions ($E \leq 3$ GeV), while we use the scaling approach given in eqs. (9) and (10) for $E_p > 7$ GeV, with $f_{\pi^0} = (1/2)f_{\pi^\pm}$.

The flux of gamma rays due to bremsstrahlung of secondary electrons is given by

$$j_{\gamma}^{brem}(E_{\gamma}, r) = n_H(r)c \int_{E_{\gamma}}^{E_p^{max}} dE_e n_e(E_e, r) \frac{d\sigma}{dE_{\gamma}}(E_e, E_{\gamma}), \quad (19)$$

where the differential cross section can be written as

$$\frac{d\sigma}{dE_{\gamma}}(E_e, E_{\gamma}) = 2.6 \cdot 10^{-26} \frac{1}{E_e} \Lambda(v) \quad cm^2 GeV^{-1}, \quad (20)$$

and the quantity $\Lambda(v)$ is:

$$\Lambda(v) = v + \frac{1-v}{v} \left(\frac{4}{3} + 2b \right) \quad (21)$$

with $b \approx 0.01$.

The total amount of gamma ray emission at energy E_{γ} from a single cluster is obtained, as usual, by volume integration:

$$J_{\gamma}(E_{\gamma}) = \int_0^{R_H} dr 4\pi r^2 j_{\gamma}(E_{\gamma}, r), \quad (22)$$

where $j_{\gamma}(E_{\gamma}, r) = j_{\gamma}^{\pi^0}(E_{\gamma}, r) + j_{\gamma}^{brem}(E_{\gamma}, r)$.

5 The case of the Coma cluster

As described in the previous sections the SEM implies that:

i) a flux of radio emission is produced due to the synchrotron emission of electrons produced in CR interactions;

ii) secondary electrons with $E \geq 1$ GeV radiate in the X-ray energy range due to ICS on the photons of the microwave background radiation;

iii) secondary electrons with $E \leq 400$ MeV produce UV photons in the energy range $E_{UV} \leq 0.4$ keV.

iv) gamma rays are copiously produced in the decays of the neutral pions.

The last point *iv)* represents, at the same time, a unique signature of the SEM and a way to impose strong constraints on this model.

In this section we analyze the predictions of the SEM for the Coma cluster and we compare them with the available data in the radio [2], hard X-ray [12] [13], UV [14,10,24] bands and with the EGRET upper limit on the gamma ray emission at $E > 100$ MeV [11].

Let us begin with the case of a single source of CR. As we stressed in Section 2, the CR diffusion coefficient, $D(E_p)$, is uncertain and there are not yet reliable constraints on its functional dependence on the CR energy. We adopt here a Kolmogorov spectrum of the fluctuations in the IC magnetic field and derive an explicit form for the diffusion coefficient, as given in eq. (2). This expression has the advantage to relate the diffusion coefficient $D(E_p)$ directly to observable quantities like the coherence length and the strength of the magnetic field, while typically these quantities are all considered as independent parameters. Following [25], we fix here $l_c = 20$ kpc, to have a conservative result. The conclusions discussed below will be strengthened for a larger value of l_c . As for the parameters of the IC gas density profile of Coma, we used $n_H^0 = 3 \cdot 10^{-3} \text{ cm}^{-3}$, $r_0 = 400$ kpc and $\beta_{IC} = 0.75$.

The diffuse radio flux for Coma has been evaluated according to eq. (13). We use the CR luminosity, L_p , as a normalization parameter and we fitted it to the observations. Once the normalization is fixed, the flux of non-thermal X-rays and gamma rays is easily calculated from eqs. (16) and (18-22). This procedure has been repeated for $\gamma = 2.1$ and $\gamma = 2.4$, which can be considered as a lower and an upper limit to the power index of the injection CR spectrum, and for three values of the magnetic field, $B = 0.1, 1$ and $2 \mu G$.

The results of our calculations for the spectrum of the radio halo of Coma are shown in Fig. 1a ($B_\mu = 0.1$), Fig. 1b ($B_\mu = 1$) and Fig. 1c ($B_\mu = 2$). The solid lines refer to $\gamma = 2.1$ and the dashed lines to $\gamma = 2.4$. The data points are taken from [2]. The CR luminosities needed to fit the radio halo data are reported in Table 1. It is evident that for large values of the IC magnetic field ($B \sim 1 - 2 \mu G$) the CR luminosities required to fit the data, $L_p \sim (0.1 - 1) \cdot 10^{44}$ erg/s (see Table 1), are of the order of the typical CR powers predicted in clusters of galaxies (see [6,7]). For low values of $B \sim 0.1 - 0.2 \mu G$, considerably larger CR luminosities, $L_p \gtrsim 5 \cdot 10^{45}$ erg/s, are required by the observations.

The allowed range of parameters is drastically reduced when the analysis is not limited to the radio halo data alone but include also the recent detection of hard X-ray tails and the existing EGRET upper limit on the gamma ray emission from Coma. Our predictions for the non-thermal X-ray emission from Coma are plotted in Fig. 2a ($B_\mu = 0.1$), Fig. 2b ($B_\mu = 1$) and Fig. 2c ($B_\mu =$

2), where the solid and dashed lines are again for $\gamma = 2.1$ and $\gamma = 2.4$, respectively. The shaded area shows the thermal bremsstrahlung continuum that fits the HEAO1-A4 and GINGA data (open triangles) with a temperature of $T = 8.21 \pm 0.20$ keV. The OSSE upper limits are indicated with open circles and the SAX data points are represented by the filled squares. The plotted errorbars refer to 90% confidence level.

From Fig. 2 it is clear that only models with small values of B_μ ($B_\mu \approx 0.1$) can reproduce the observed X-ray flux in the energy region between 20 keV and 100 keV, while the contribution of the secondary electrons to the X-ray flux for larger values of B_μ is negligible. The interpretation of this result is straightforward: in fact, contrary to the diffuse radio flux, the X-ray flux is very weakly dependent on the value of the magnetic field [see eq.(13)]. Specifically, it depends on B_μ mainly through the normalization of the CR spectrum that is required to fit the radio halo data. Therefore, low values of B_μ imply large CR luminosities L_p (because of the low radio emissivity) and, in turn, large X-ray fluxes. On the other hand, for large values of B_μ electrons radiate more efficiently and low values of L_p are needed, which in turn imply low X-ray fluxes.

Recently, also UV emission was detected from Coma [14], and interpreted as ICS of electrons with energy between 150 MeV and 400 MeV [10,24]. In the SEM the flux of UV emission due to ICS crucially depends on the CR injection spectrum below ~ 1 GeV, which is poorly known and may reflect specific conditions in the acceleration region. The spectrum of secondary electrons in the energy range of interest suffers a substantial flattening due to the peculiar shape of the pion spectrum at low energy and due to Coulomb energy losses. In the assumption, used in this paper, of a CR spectrum which is a power law in momentum, our prediction of the UV flux for $B_\mu \sim 0.1$ falls short of the observed flux [14] by a factor 1.5 – 2.

Values $B_\mu \sim 0.1$ in the Coma ICM are consistent with the findings of [12]. However, in the SEM this result has further implications: in cases where the X-ray emission becomes appreciable (*i.e.* for low values of B_μ) with a large L_p needed, the gamma ray emission predicted for Coma on the basis of eqs.(16-19) grows linearly with L_p and the gamma ray flux very easily exceeds the EGRET limit as shown in Table 1, where the fourth column represents the ratio of the flux predicted in the SEM to the EGRET upper limit from Coma, $F_\gamma^{EGRET}(E > 100\text{MeV}) \approx 4 \cdot 10^{-8} \text{ photons } s^{-1} \text{ cm}^{-2}$. The contribution of secondary electron bremsstrahlung to the gamma ray emission of Coma is always negligible with respect to the contribution of gamma rays produced by neutral pion decay (we report the ratio of the two contributions in the last column of Table 1).

Our predictions for the differential gamma ray spectra from Coma are plotted

in Fig. 3a ($B_\mu = 0.1$), 3b ($B_\mu = 1$) and 3c ($B_\mu = 2$). The thick lines are the contributions of π^0 decay while the thin lines represent the bremsstrahlung gamma rays from the secondary electrons. The solid and dashed lines are, as usual, for $\gamma = 2.1$ and $\gamma = 2.4$ respectively.

How much does this conclusion depend upon the assumption of a single source of CR? In order to answer this question we evaluate the fluxes of radio and hard X-rays for a homogeneous injection of CR over the cluster volume. If the observed radio halo spectrum at $\nu \leq 1.4$ GHz is taken as a power law with power index $\alpha_r = 1.16$ [9], then the best fit to the data is obtained for $\gamma = 2\alpha_r = 2.32$. We use eq. (5) for the equilibrium proton distribution in the ICM and the results of Section 3 to determine the relative spectra of secondary electrons. Radio, X-ray and gamma ray fluxes are calculated as usual.

The comparison with the radio [2] and hard X-ray [12] data yields $\epsilon_{tot} \approx 8 \cdot 10^{63}$ erg and $B_\mu \approx 0.1$. The value of ϵ_{tot} corresponds, if averaged over the age of the cluster, to a huge CR luminosity of $L_p \sim 2 \cdot 10^{46}$ erg/s. The gamma ray flux which corresponds to this value of ϵ_{tot} is $F_\gamma(E_\gamma > 100 \text{ MeV}) \approx 1.2 \cdot 10^{-7} \text{ cm}^{-2} \text{ s}^{-1}$, which exceeds the EGRET limit on Coma by a factor ~ 3 .

Thus, our conclusion can be stated as follows: if the radio and X-ray non-thermal fluxes are due to synchrotron and ICS of the same population of secondary electrons, then the SEM cannot fit the two sets of observations without exceeding the EGRET limit. In this case and within the assumptions used in this paper, the SEM can be ruled out already on the basis of the present data.

Is there any way to mitigate the strength of this result? We can envision two possible avenues: from the point of view of data analysis, it was already pointed out in [12] that the rebinning of the hard X-ray data according with the OSSE energy binning yields an hard X-ray flux which is a factor ~ 2 below the OSSE upper limit at $E \geq 40$ keV. This allows the magnetic field to increase to values $B_\mu \approx 0.15 - 0.2$ and the corresponding gamma ray fluxes to decrease slightly below the EGRET limit for $\gamma \approx 2.1$, or slightly above it for $\gamma = 2.4$.

From the theoretical point of view, the ICS origin of the hard X-ray excess observed in Coma cannot be taken for granted as pointed out in [26]. The previous authors propose, in fact, that the turbulence in the ICM may be able to accelerate stochastically a fraction of thermal electrons producing a non-thermal tail of the electron distribution without appreciably change the energy budget of the electrons in the IC gas. Such non-thermal tail can easily reproduce the SAX data through bremsstrahlung emission. The main consequence of this is that the hard X-ray flux becomes completely decoupled from the radio halo flux and no constraint on the strength of the IC magnetic field

can be derived. Therefore, the large B_μ field solutions illustrated in Figs. 1b and 1c may well fit the radio spectrum and contribute only very marginally to the hard X-ray spectrum. In this case the gamma ray flux for Coma predicted by the SEM is well below the EGRET limit.

As for the UV flux, the small discrepancy we found might be due to the specific choice of the CR spectrum at low energy. In any case, the origin of the UV excess is still under debate, and a thermal contribution cannot be excluded (see discussion in [27]).

We did not discuss here the additional issue concerning the nature of the claimed steepening in the radio halo spectrum at frequencies > 1.4 GHz. Whether this is a real feature or an instrumental artifact is not yet clear (see discussion in [9]). However, if future measurements will confirm this result, the SEM will again have problems since the electron ageing, often invoked to describe the steepening of the spectrum, is not effective in the SEM because secondary electrons are continuously produced through CR interactions and replenish the radio halo spectrum, even if the CR source is no longer active. On the other hand, the SEM predicts a steepening of the radio spectrum at high frequency, where CR begin to be not confined by the IC magnetic field (see Section 4.1 for details), but at present such a steepening does not seem sufficient to reproduce the data at $\nu \gtrsim 2.7$ GHz, assuming that these results are not due to any instrumental bias.

6 Discussion and conclusions

In this paper, we calculated the spectra of the non-thermal radio, X-ray, UV and gamma ray emission expected from clusters of galaxies in the context of the secondary electron model, and we compared our predictions to the available data for the Coma cluster. The calculations have been carried out in the case of a single source of CR and in the case of a homogeneous injection of CR in the ICM.

For the case of a single CR source and adopting a Kolmogorov spectrum of the magnetic fluctuations in the ICM, the radio data between 30 MHz and 1.4 GHz can be fitted in the context of the SEM for a wide range of values of the parameters (specifically the value of the magnetic field and the spectrum of the injected CR). In particular, for magnetic fields of the order of $1 - 2 \mu G$ the CR luminosities needed to fit the radio data are completely consistent with the presence of ordinary sources of CR in clusters, as considered in [6] ($L_p \leq 10^{44}$ erg/s).

Moreover the model has the noticeable property that electrons are produced

in situ at any time, so that there is no need for a reacceleration mechanism which is necessary in the primary electron model in order to make it possible for electrons to reach distances of ~ 1 Mpc (the scale of the Coma radio halo) without appreciable energy losses.

Together with the diffuse radio emission, non-thermal X-rays (due to ICS of secondary electrons) and gamma rays (mainly due to neutral pion decay and to bremsstrahlung of secondary electrons) are produced.

The comparison of our predictions with the available X-ray and gamma ray data allows us to put strong constraints on the SEM as a plausible explanation for the origin of the radio halos in Coma-like clusters. In fact, if the X-ray emission is due to ICS of the same electron population which is responsible for the diffuse radio emission, then low values of the magnetic field ($B_\mu \sim 0.1$) and correspondingly large CR luminosities ($L_p \gtrsim 5 \cdot 10^{45}$ erg/s) are required, which in turn imply a flux of gamma rays at $E_\gamma \geq 100$ MeV exceeding the EGRET limit by a factor ~ 2 for a power index of the injection spectrum of CR $\gamma = 2.1$, and by a factor ~ 7 for $\gamma = 2.4$.

This result requires some more comments: assuming a cluster temperature of $T = 8.21$ keV, and a typical IC gas density in the inner ~ 1 Mpc of the cluster of $n_H \sim 10^{-3} \text{ cm}^{-3}$, the total thermal energy in the cluster can be estimated to be $\epsilon_{th} \sim 2 \cdot 10^{63}$ erg. Now, if we follow [24] in requiring equipartition between thermal and non-thermal energy in the ICM, this translates into a CR luminosity, averaged over the age of the cluster, of $L_p^{eq} \sim 5 \cdot 10^{45}$ erg/s, which is of the same order of the CR luminosities required in the SEM to reproduce the radio and hard X-ray emission from Coma. However, as we have shown in Section 5, in this case the corresponding gamma ray luminosities contributed by pion decay can very easily exceed the EGRET limit or fall short of this limit by a very small amount. This conclusion is not changed if a homogeneous injection of CR in the ICM is assumed, as discussed in Section 5.

Though this is not enough to rule out the possibility of CR in equipartition in clusters like Coma, it certainly represents a strong constraint on this possibility. The next generation gamma ray satellites (INTEGRAL, GLAST) will answer this question definitely. In fact, future gamma ray observations will tell us not only the flux of gamma rays but also the nature of the process responsible for that: specifically, if the bulk of gamma rays comes from pion decay in the ICM, there is a unique signature, represented by a bump in the gamma ray spectrum at ~ 70 MeV (see Fig. 3).

Is there an alternative way of interpreting the combined radio and hard X-ray data that does not require equipartition CR energy densities? It was recently proposed in [26] that the hard X-ray flux from Coma can as well be interpreted as bremsstrahlung emission from a supra-thermal electron tail developed in

the thermal electron distribution due to stochastic acceleration in the turbulent ICM. Clearly, these last electrons are not relevant for the radio halo emission, so that a non-thermal population of electrons in the GeV energy range is required. If this will turn out to be the explanation of the hard X-ray excess of Coma, then the observed radio and non-thermal X-ray fluxes are no longer strictly related. As a consequence, the radio halo emission can be produced by a population of secondary electrons radiating in a $B \sim 1\mu G$ average magnetic field, without overproducing gamma rays (see Table 1) and giving a marginal contribution to the non-thermal X-ray flux by ICS.

In any case, it is important to realize that the gamma ray limit, widely discussed in this paper, appears to be relevant whatever the process of production of the radiating electrons is. Therefore, the EGRET upper limit must be considered as binding in the SEM, as well as in other models for the non-thermal processes in clusters of galaxies, whenever large CR energy densities are invoked. This aspect was also recognized in [24] but the importance of the gamma rays from pion decay was largely underestimated.

Finally, we want to discuss briefly the problem of the rarity of the radio halos in clusters of galaxies. This problem needs a definitive explanation in every model for the origin of radio halos. At present, only half a dozen clusters have been shown to have prominent radio halos (see [28] for a review) and it is natural to look for the reason for such a rarity. Most of the radio halo clusters have high temperatures ($T \gtrsim 7$ keV) and X-ray luminosities $L_X \gtrsim$ a few 10^{44} erg/s and show evidences of recent merging (Coma [29], A2319 [30], A2163 [31], A2218) and/or of non-thermal pressure support of their IC medium (A85 [32])

There are a number of factors that can play a relevant role: first of all, the CR injection in the ICM depends on the morphology of the cluster (e.g. on the number of active galaxies in a cluster) and on the history of the cluster (e.g. on the occurrence of recent mergings). Thus, it is conceivable that only a few clusters have powerful CR sources operating for long enough in the ICM to provide high powers in accelerated particles. Secondly, the different physical conditions present in the ICM determine quite a variety of values for the magnetic field and for the diffusion coefficient. In fact, we have shown in this paper that, at fixed L_p , changing the average IC magnetic field from $1\mu G$ to $0.1\mu G$ decreases the radio halo flux by a factor $\gtrsim 100$, so that very weak radio halos can fall below the sensitivity threshold of the current experiments.

The origin of radio halos is, in our opinion, strictly related to the mechanism of production of the high energy electrons and to the physical mechanisms which create the environment in which they radiate, and can hardly be envisioned at the present stage of observations. The combination of the next generation, high-sensitivity radio, soft and hard gamma ray experiments will provide a

zoo of non-thermal phenomena in galaxy clusters and will hopefully shed a new light on this problem.

Aknowledgements

We are grateful to an anonymous Referee for his comments and suggestions which allowed us to improve considerably the presentation of the paper. The research of PB is funded by a INFN fellowship at the University of Chicago. S.C. also acknowledges useful discussions with L. Feretti, G. Giovannini and R. Fusco-Femiano.

References

- [1] L. Feretti and G. Giovannini 1997, Contribution to the Rencontres Astrophysiques International Meeting "A New Vision of an Old Cluster: Untangling Coma Berenices", eds. F. Durret et al., held in Marseille, France 17-20 June 1997 (astro-ph/9709294).
- [2] G. Giovannini, L. Feretti, T. Venturi, K.-T. Kim and P.P. Kronberg 1993, *Astrophys. J.*, 406, 399.
- [3] B. Dennison 1980, *Astrophys. J.*, 239, L93.
- [4] W.T. Vestrand 1987, ICRC Proceedings, OG 3.1-5, 97.
- [5] A. Dar and N.J. Shaviv 1995, *Phys. Rev. Lett.* 75, 30, 52
- [6] V.S. Berezhinsky, P. Blasi and V. Ptuskin 1997, *Astrophys. J.*, 487, 529.
- [7] S. Colafrancesco and P. Blasi 1998, *Astropart. Phys.*, 9, 227
- [8] X. Chi, E.C.M. Young, P.K.N. Yu, L. Zhang and Q-Q. Zhu 1996, *Phys. Rev. Lett.*, 77, 1436.
- [9] R.M. Deiss, W. Reich, H. Lesch and R. Wielebinski 1977, *A&A*, 321, 55.
- [10] S. Bowyer and T.W. Berghöfer 1998, *Astrophys. J.*, 506, 502
- [11] P. Sreekumar, et al. 1996, *Astrophys. J.*, 464, 628
- [12] R. Fusco-Femiano, et al. 1999, preprint astro-ph/9901018
- [13] Y. Rephaeli, D. Gruber and P. Blanco 1999, *Astrophys. J.*, 511, L21
- [14] Lieu, R. et al. 1996, *Science*, 274, 1335
- [15] V. Quilis et al. 1998, preprint astro-ph/9803059
- [16] U. Briel and P. Henry, 1997, preprint astro-ph/9711237
- [17] P. Blasi and S. Colafrancesco 1999, *in preparation*
- [18] K.-T. Kim, P.P. Kronberg, P.E. Dwedney and T.L. Landecker 1990, *Astrophys. J.*, 355, 29.
- [19] P.P. Kronberg 1994, *Rep. Prog. Phys.*, 57, 325.
- [20] C.L. Sarazin 1988, *X-ray Emission from Clusters of Galaxies*, Cambridge University Press, Cambridge.
- [21] C.D. Dermer 1986, *A&As*, 157, 223.
- [22] A.W. Strong and I.V. Moskalenko 1998, *Astrophys. J.*, 493, 694.
- [23] M.S. Longair 1994, *High Energy Astrophysics*, Cambridge University Press, Cambridge.

- [24] R. Lieu, W.H. Ip, W.I. Axford and M. Bonamente 1998, preprint astro-ph/9809175, *Astrophys. J.* in press
- [25] W.J. Jaffe 1980, *Astrophys. J.*, 241, 924
- [26] T.A. Ensslin, R. Lieu and P. Biermann, preprint astro-ph/9808139.
- [27] Arabadjis, J.S. & Bregman, J.N. 1998, preprint astro-ph/9810377
- [28] L. Feretti and G. Giovannini 1996, in *Extragalactic radio Sources*, IAU Symp. No 175, Eds. R.Ekers et al., p.333
- [29] U.G. Briel, J.P. Henry and H. Boheringer 1992, *A&A*, 259, L1
- [30] L. Feretti, G. Giovannini and H. Boheringer 1997, *New Astronomy*, 2, 501
- [31] M. Markevitch, et al. 1996, *Astrophys. J.*, 456, 437
- [32] A. Loeb and S. Mao 1994, *Astrophys. J.*, 435, L109
- [33] Y. Rephaeli, M. Ulmer and D. Gruber 1994, *Astrophys. J.*, 429, 554
- [34] J.P. Hughes, J.A. Butcher, G.C. Stewart and Y. Tanaka 1993, *Astrophys. J.*, 404, 611

Table 1
 Summary of the fitting parameter values

B_μ	γ	$\frac{L_p}{10^{44} \text{ ergs}^{-1}}$	$\frac{F_\gamma(E_\gamma \geq 100 \text{ MeV})}{F_\gamma^{EGRET}(E_\gamma \geq 100 \text{ MeV})}$	$F_\gamma^{brem} / F_\gamma^{\pi^0}$
0.1	2.1	50	1.93	0.13
0.1	2.4	180	7.15	0.10
1	2.1	0.35	$1.8 \cdot 10^{-2}$	0.14
1	2.4	1	$4.5 \cdot 10^{-2}$	0.11
2	2.1	0.1	$5.3 \cdot 10^{-3}$	0.12
2	2.4	0.23	$1.1 \cdot 10^{-2}$	0.095

Figure captions

Figure 1 Spectrum of the diffuse radio emission from the Coma cluster for different values of the average intracluster magnetic field: $B = 0.1 \mu G$ (left panel), $B = 1 \mu G$ (central panel) and $B = 2 \mu G$ (right panel). A King density profile has been used with $\beta_{IC} = 0.75$, $n_H^0 = 2.89 \cdot 10^{-3} \text{ cm}^{-3}$ and $r_c = 0.42$ Mpc (we use here $h = 1/2$). For each panel the cases $\gamma = 2.1$ (continuous curves) and $\gamma = 2.4$ (dashed curves) are shown. The parameters that best fit the data in each figure are listed in Table 1 and are obtained fitting the radio halo data at $\nu \gtrsim 30$ MHz. Data points are taken from [2].

Figure 2 Spectrum of the diffuse X-ray emission from Coma. The three panels refer to the same values of the IC magnetic field as in Fig. 1. The shaded area shows the best fit to the HEAO1-A4 and GINGA thermal emission data (open triangles) at $T = 8.21 \pm 0.20$ keV [34]. The OSSE upper limits [33] are indicated by the open circles. The SAX data [12] are indicated by filled squares. Arrows and labels show, for each panel, the energy ranges in which the three different data sets are located. Predictions of the SEM for $\gamma = 2.1$ (continuous curves) and $\gamma = 2.4$ (dashed curves) are shown in each panel.

Figure 3 The predicted differential gamma ray spectra from Coma, in the SEM. The three panels refer to the values of the magnetic field indicated. The thick lines represent the contribution of neutral pion decay, while the thin lines represent the bremsstrahlung contribution of secondary electrons. Solid and dashed curves are for $\gamma = 2.1$ and $\gamma = 2.4$ respectively.

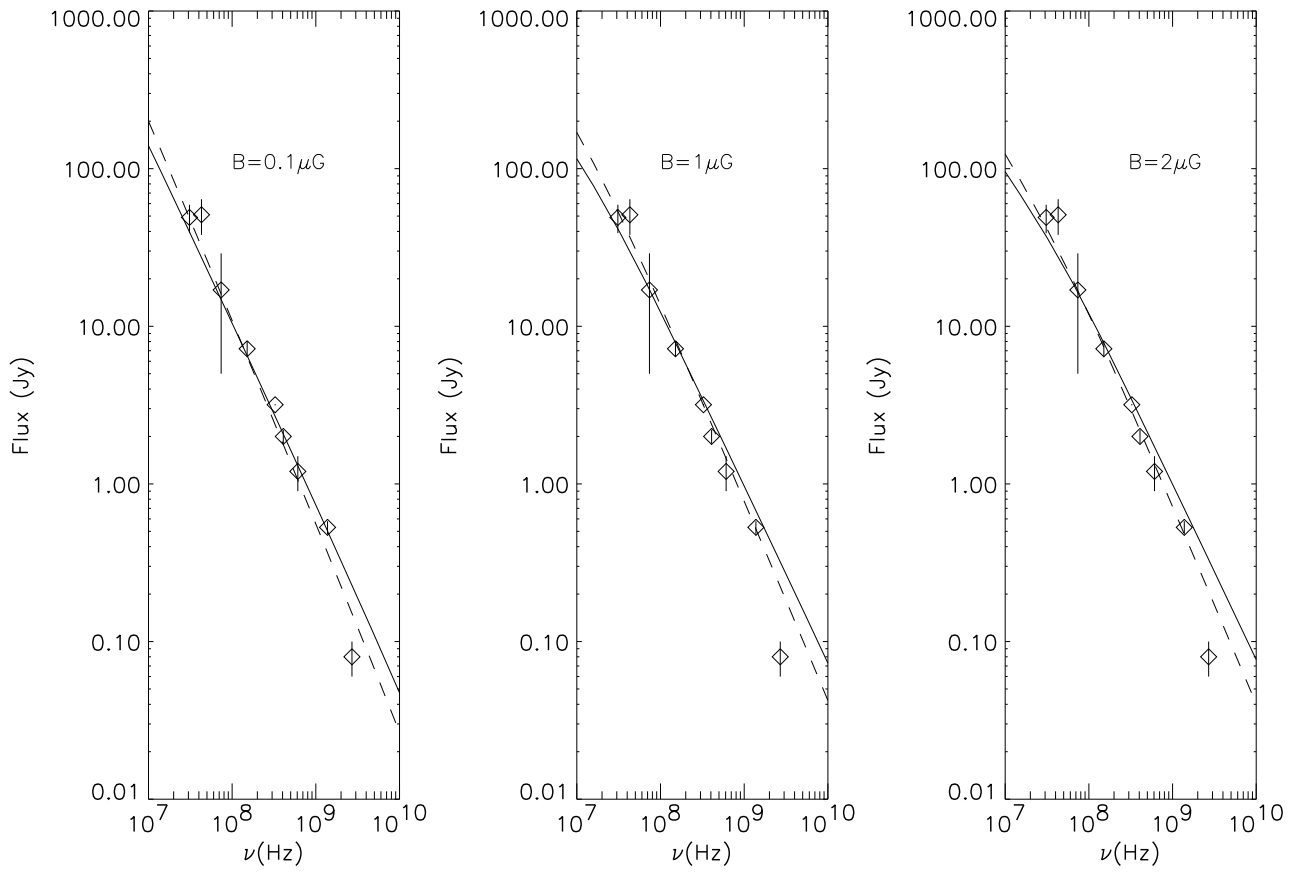


Fig. 1.

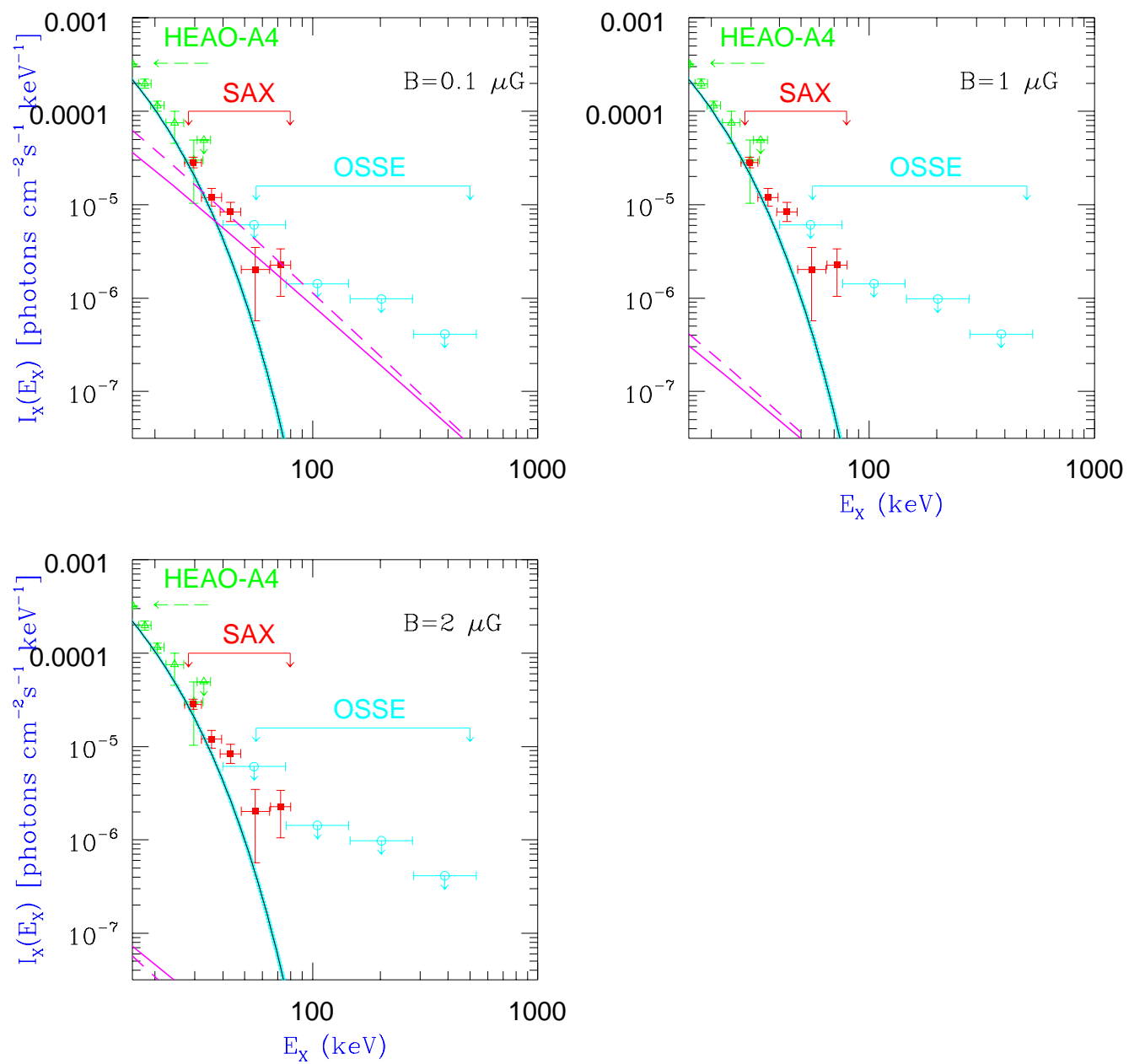


Fig. 2.

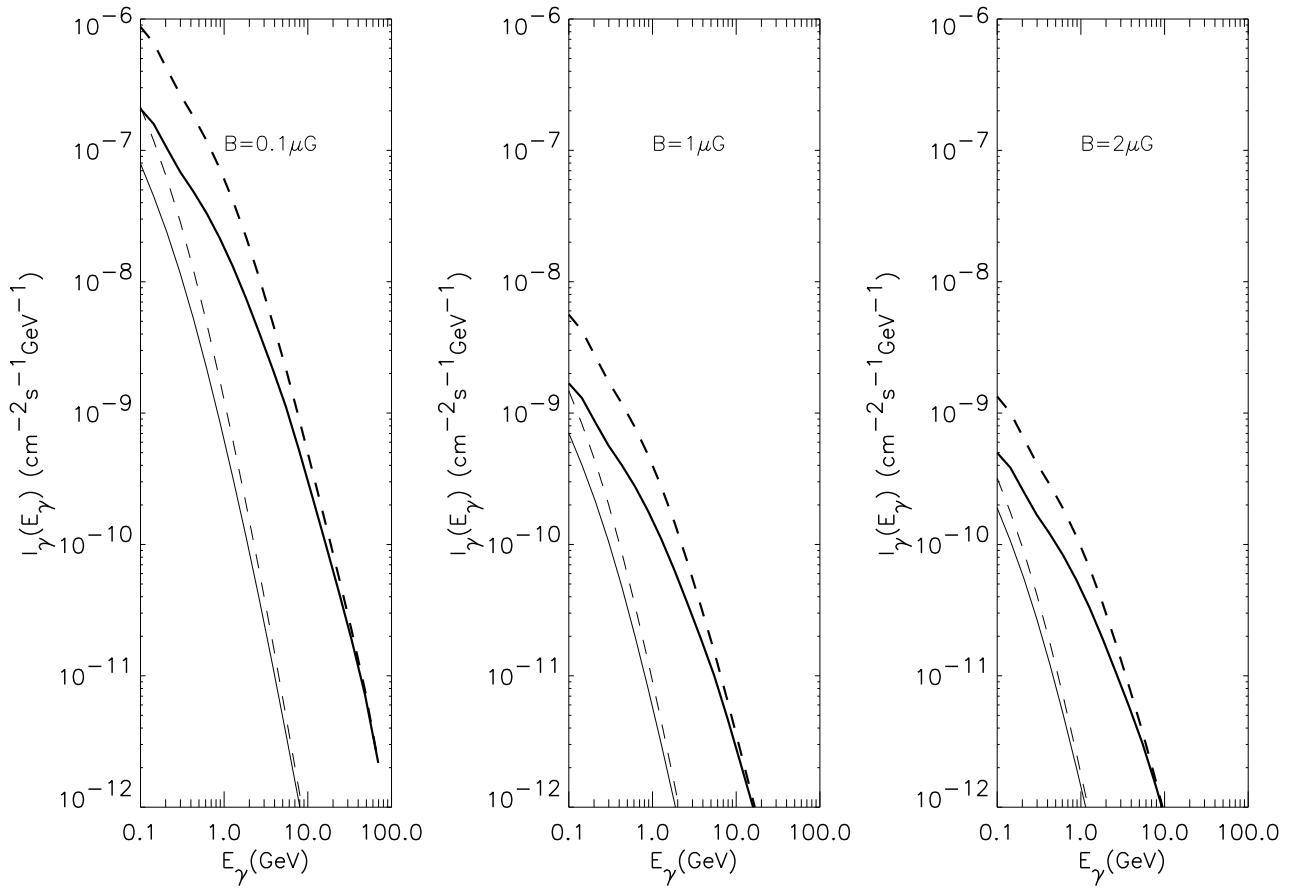


Fig. 3.